J. Fluid Mech. (2006), *vol.* 555, *pp.* 439–458.
doi:10.1017/S0022112006009323 Printed in the United Kingdom

On the dynamics of the large-scale structures in round impinging jets

By J.W. HALL† AND D. EWING

Department of Mechanical Engineering, McMaster University, Hamilton, ON, L8S 4L7, Canada

(Received 21 March 2005 and in revised form 28 October 2005)

Time-averaged two-point measurements of the fluctuating wall pressure and instantaneous measurements of the full fluctuating wall pressure field were performed in incompressible turbulent impinging jets with nozzle-to-plate spacings of 2 and 4 diameters, Reynolds numbers of 23 300, and Mach numbers of 0.03. An azimuthal Fourier decomposition of the fluctuating wall pressure revealed that the fluctuations in the stagnation region were dominated by azimuthal mode 1 to 3, and the contributions from these modes were larger for the jet with $H/D = 4$. Azimuthal modes 0 and 1 made significant contributions to the pressure fluctuations in the wall jet region of both jets, indicating that the large-scale ring structures formed in the jet shear-layer play a prominent role in this region. The contributions from modes 0 and 1 in the wall jet were smaller for the jet with $H/D = 4$ indicating that the ring structures play a less prominent role in the wall jet region as the nozzle-to-plate distance increased. A wavelet analysis of the transient fluctuations indicated that azimuthal mode 1 had dominant high-frequency and low-frequency components, while azimuthal mode 0 had only the higher-frequency oscillations. The higher-frequency components of azimuthal modes 0 and 1 occurred in both the stagnation and the wall jet regions and are attributed to the asymmetric evolution of the ring structures in the jet. The low-frequency oscillations were primarily associated with azimuthal mode 1 and were evident only in the stagnation region. These oscillations became more prominent as the nozzle-to-plate distance was increased.

1. Introduction

There have been numerous investigations of the flow field (e.g. Cooper *et al.* 1993; Fairweather & Hargrave 2002) and heat transfer (e.g. Viskanta 1993; Webb & Ma 1995) produced by turbulent round impinging jets, motivated in part because impinging jets occur widely in practical applications such as electronics cooling and vertical stationary take off/landing aircraft (VSTOL). The development of the impinging jet flow field is typically divided into two regions, the stagnation region associated with the turning of the mean flow, $r/D < 1$, and the radial wall jet region, $r/D > 1$. It is increasingly recognized that the large-scale structures formed in the jet shear-layer play an important role in the flow and heat transfer produced by the round impinging jet in both regions. For example, when the jet nozzle is approximately 6 diameters from the surface, the collapse of the impinging jet's potential core causes large-scale turbulent fluctuations near the wall that enhance the heat transfer in the stagnation region (cf. Kataoka *et al.* 1982, 1987). In round jets with smaller

† Present Address: Department of Mechanical and Aerospace Engineering, Syracuse University, Syracuse, NY, 13244, USA; jhall04@syr.edu.

nozzle-to-plate distances, the quasi-periodic vortex ring structures formed in the jet shear-layer impinge on the wall and then spread radially outward causing an unsteady separation in the radial wall jet (Didden & Ho 1985; Landreth & Adrian 1990), similar to that observed when a vortex ring interacts with a wall (e.g. Walker *et al.* 1987; Doligalski, Smith & Walker 1994). The ring structures impinging on the surface play an important role in the resonant feedback mechanism in compressible impinging jets (Ho & Nosseir 1981; Nosseir & Ho 1982), while the unsteady separation in the radial wall jet seems to cause a secondary peak in the heat transfer in this region (Viskanta 1993; Webb & Ma 1995).

The unsteady separation in the radial wall jet formed by a forced impinging round jet was examined in detail by Didden & Ho (1985). They observed that the vortex rings formed in the jet shear-layer approach the plate approximately 0.9 diameters from the jet centreline and then travel radially outward over the surface causing the formation of secondary vortex rings near the wall. These secondary vortex rings eventually were ejected from the surface approximately 1.5 diameters from the jet centreline. They then wrapped around the primary rings which led to the breakdown of both ring structures. Popiel & Trass (1991) and Landreth & Adrian (1990) observed a similar unsteady separation process in unforced round impinging jets using flow visualization and particle image velocimetry (PIV) measurements, respectively, whereas Gogineni & Shih (1997) observed similar events in the near field of a two-dimensional planar wall jet. In the latter case, the large-scale structures in the jet's outer shear-layer caused an unsteady separation of the near-wall layer.

Landreth & Adrian (1990) noted that the development of the primary and secondary vortex structures were not symmetric about the centreline in the unforced round impinging jet. Tsobokura *et al.* (2003) observed an asymmetric tilting of the vortex ring structures approaching and interacting with the wall in a low-Reynolds-number large-eddy simulation (LES) of a forced impinging jet. The three-dimensionality of the structures in the radial wall jets formed by round impinging jets with $H/D = 2$ was examined by Hall & Ewing (2005) using two-point correlations of the fluctuating wall pressure. They found that azimuthal modes 0 and 1 made similar contributions to the fluctuating wall pressure indicating that the structures in the wall jet were asymmetric. Measurements were not reported in the stagnation region, so it was not possible to determine whether the contribution from azimuthal mode 1 was caused by oscillations in the jet shear-layer before it impinges on the wall, similar to those observed by Kataoka *et al.* (1982) for impinging jets with $H/D = 6$, or was due to asymmetries in the interaction of the vortex ring structures observed in the LES simulation of a forced jet with $H/D = 9$ by Tsobokura *et al.* (2003).

The interaction of the large-scale structures with the surface in round impinging jets changes as the distance between the nozzle and the surface is increased, and is probably related to the known downstream breakdown of the the large-scale structures in the axisymmetric shear-layer (Liepmann & Gharib 1992; Citriniti & George 2000; Jung, Gamard & George 2004). The effect of this change can be seen in measurements of the heat transfer (e.g. Viskanta 1993; Webb & Ma 1995). In particular, the secondary peak in the heat transfer present in the wall jet region decreases and disappears when the nozzle-to-plate spacing is increased from approximately 2 to 6 diameters. The heat transfer in the stagnation regions increases as the nozzle-to-plate distance increases over this range, indicating that the changes in the structures affect the flow in the stagnation region and wall jet region differently.

The present work examines the relationship between the large-scale structures present in the stagnation region and the wall jet region of an impinging jet flow. The

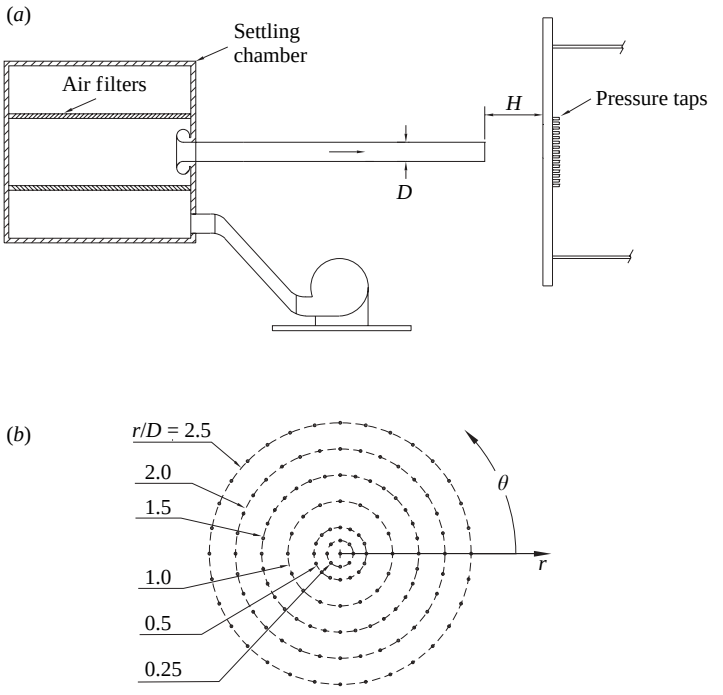

FIGURE 1. Schematics of (*a*) the experimental apparatus and (*b*) the pressure taps on the impingement surface where the circles represent the pressure taps.

measurements were performed for impinging jets with nozzle-to-plate distances of 2 to 4 diameters to examine how this relationship changes when this distance is varied. This was not intended as a comprehensive investigation of the effect of the nozzle-to-plate distance but, as shown below, it has provided considerable insight into this effect. The development of the structures in the wall jet region were initially examined using two-point correlation measurements of the fluctuating wall pressure. Following this, the development of the instantaneous structures in the jets were characterized using simultaneous time-resolved measurements of the fluctuating pressure field on the surface. The experimental apparatus and methodology used in this investigation are described in § 2. The two-point and two-time correlation measurements and instantaneous measurements of the fluctuating pressure are then presented in § 3. Finally, the results are discussed and conclusions presented in § 4.

2. Experimental facility

The experimental apparatus used in this investigation, and used previously by Hall & Ewing (2005), is shown in figure 1. The impinging jet exits a long pipe with a diameter, D, of 38.1 mm and a length of 60 diameters. The air flow was supplied by a 5 h.p. variable speed blower and was conditioned using a series of 460 mm diameter circular filters mounted in a large $760 \times 760 \times 760\,\mathrm{mm}^3$ settling chamber. The flow then entered the long pipe through a machined bellmouth. Sun (2002) and Gao, Sun & Ewing (2003) measured the mean streamwise velocity and the streamwise turbulence intensity at the pipe exit using hot-wire anemometry for Reynolds numbers ranging from 23 000 to 110 000. The mean profiles were in good agreement with the profiles for

fully developed turbulent pipe flow, and the flow exiting the pipe was axisymmetric. The measurements of the impinging jet were performed here for jets with centreline velocities of 11.7 m s^{-1} corresponding to a bulk velocity, $U_o = Q/A$, (based on a 1/7 profile) of 9.54 m s^{-1} and a Reynolds number of 23 300.

The jet impinged onto a stiff smooth 10 mm aluminium tooling plate that was 92 cm $\times$ 92 cm^2. The plate was rigidly mounted on a traverse that could be used to adjust the position of the plate relative to the jet outlet. Following the approach used by Ho & Nosseir (1980), Kataoka *et al.* (1982) and Hall & Ewing (2005), the development of the large-scale structures in the impinging wall jet was examined by measuring the fluctuating wall pressure. Here, the pressure was measured at 6 concentric rings of pressure taps at $r/D = 0.25$, 0.5, 1.0, 1.5, 2.0 and 2.5 and a lone tap positioned at the jet centreline (figure 1*b*). These rings contained 8, 16, 16, 32, 32 and 32 equally spaced flush-mounted taps with an inner diameter of 1.2 mm. The taps not in use were plugged on the back of the plate using a closed piece of Tygon tubing.

The development of the structures in the wall jet region was first examined using measurements of the two-point and two-time correlations of the fluctuating wall pressure. These correlations were measured using two microphones that were moved between the taps. The instantaneous dynamics of the structures in the flow were then examined by simultaneously measuring the fluctuating pressure at all the points using a multi-channel pressure transducer system. The details of the two measurements are outlined below. The statistical measurements from the two approaches were compared and found to be in good agreement (cf. Hall *et al.* 2003). The microphone measurements had a greater dynamic range and are thus used for most of the statistical measurements presented here.

2.1. *Microphone measurements*

The two-point and two-time correlations of the fluctuating wall pressure were measured using two Sennheiser microphones housed in snugly fitting Delron cases that included 1.2 mm diameter taps on the tops of the cases. The taps on the microphone cases were connected to the pressure taps on the plate using 40 mm long Tygon tubes. The response of the Sennheiser microphones was flat for frequencies between 35 and 10 000 Hz. The experimentally determined resonant frequencies of the measurement systems were over 2 500 Hz, well above the frequencies of interest here. The linear sensitivity coefficients of the microphones were determined by calibrating the microphones using a B&K pistonphone.

The voltage signals from the two microphones were recorded using two channels on an 8 channel, 16 bit Microstar 1816 A/D board that included passive high-pass anti-aliasing filters and on-board digital filters for each channel. The digital filters for the two channels were set to be constant-phase brick-wall low-pass filters with cutoff frequencies of 2300 Hz for the measurements reported here. The filtered voltage signals from the two microphones were sampled in 100 blocks of 1200 data points at 4800 Hz. The sampled signals were then converted to instantaneous pressures using the linear sensitivity coefficients of the microphones. The mean pressure for the full record from each channel was subtracted from the record of the instantaneous pressure, $\tilde{p}$, to compute a record of the fluctuating pressure, p. The time records were then Fourier transformed and used to compute cross-spectra. The cross-spectra for the different azimuthal separation distances were then Fourier transformed in the azimuthal direction to compute the azimuthal frequency spectra, as discussed in Hall & Ewing (2005).

The two-point and two-time correlation of the fluctuating pressure in the azimuthal direction was first measured on each of the radii between $r/D = 1.0$ and 2.5, with one

microphone at a fixed azimuthal position while the second was moved to different azimuthal positions. The symmetry of the flow was checked by comparing the standard deviation and the spectrum of the fluctuating pressure at the different azimuthal positions on each radius. It was found that the standard deviations measured at the different points on each radius agreed to within $\pm 5\,\%$ and the magnitude of the spectra agreed to within $\pm 20\,\%$, the 95 % confidence interval for the spectra. The two-point and two-time correlations were then measured between the different radial positions between $r/D = 1.0$ and 2.5. Measurements were performed for jets with $H/D = 2, 3$ and 4. The results for $H/D = 2$ and 4 are presented here. The results for the jet with $H/D = 3$ fell between the results for the other two jets and are not included here, but were presented in Hall, Gao & Ewing (2002).

2.2. *Multi-channel pressure transducer measurements*

In a later experiment performed at the boundary-layer wind-tunnel facility at the University of Western Ontario, the fluctuating pressure was measured simultaneously at all pressure taps using 9 ESP model 16TL pressure transducers that were then multiplexed using a specially designed A/D system. The pressure taps were connected to the pressure transducers through long tubes so the dynamic frequency response of the tubes and the system were calibrated before the experiment by sweeping the pressure transducers with a fluctuating pressure signal. The resulting transfer functions were used to correct the instantaneous pressure measurements. The corrected response of the sampling system was flat for frequencies between approximately 10 Hz and 400 Hz. The signals from the transducers were sampled at 800 Hz (the limit of the A/D system) in a single 180 second block. The Nyquist frequency for these measurements of 400 Hz corresponds to a non-dimensional frequency, $f_N D/U_o$, of 1.6, which was sufficient to resolve the contributions from the large-scale motions of interest here. The fluctuating pressure was again determined by subtracting the mean of the entire time record from each channel. The record was then parsed into 350 independent blocks of 400 points that were used to compute the spectra of the fluctuating pressure. The 95 % confidence interval in the estimator of the spectrum at each point was approximately 10 %. The frequency spectra, azimuthal spectra, and azimuthal frequency spectra of the fluctuating pressure from these measurements were compared to the measurements from the microphones (cf. Hall *et al.* 2003). There was approximately 10 % more energy in azimuthal modes 0 and 1 for the pressure transducer measurements. Overall, though, there was quite good agreement between the azimuthal and frequency spectra determined from the pressure transducer and microphone measurements, indicating that the time-resolved simultaneous measurements using the pressure transducers accurately captured the pressure changes on the wall. The measurements in this case were performed for jets with $H/D = 2$ and 4.

3. Experimental results

3.1. *Time-averaged statistics*

The distributions of the standard deviation of the fluctuating pressure, σ_p, measured on the wall are shown in figure 2. The results indicate that the change in the pressure fluctuations in the stagnation region and the wall jet region differed as the distance between the nozzle and the plate varied. The pressure fluctuations in the stagnation region increase in magnitude as the distance of the nozzle from the wall increases. The pressure fluctuations were largest at $r/D = 0.5$ below the nominal location of the shear-layer, and smaller in the region below the core of the impinging jet. In the wall jet region, the pressure fluctuations decreased in magnitude as the distance of the

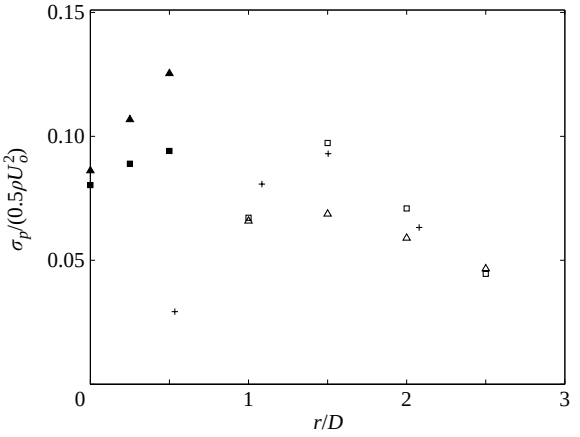

FIGURE 2. Variation in the fluctuating wall pressure for the impinging jets with □, $H/D = 2.0$, and △, $H/D = 4.0$ and $Re = 23\,300$ measured with the microphones (open symbols) and with the pressure transducers (filled symbols); and +, for a semi-compressible impinging jet with $H/D = 2.0$ and $Re = 180\,000$ from Ho & Nosseir (1980).

nozzle from the plate increased. In both cases, the pressure fluctuations in the wall jet region were initially significantly smaller than in the stagnation region. The pressure fluctuations increased to a maximum at $r/D = 1.5$ before decreasing, similar to the results by Ho & Nosseir (1980). Didden & Ho (1985) observed in their measurements of the forced impinging jet that the increase in the magnitude of the fluctuating pressure in the wall jet region was associated with the formation of secondary vortices induced by the passage of primary rings over the wall. The decrease in the pressure fluctuations after the maximum were associated with the ejection or lifting of the secondary vortices. If this is the case, the results here suggest the large-scale structures were playing a less prominent role in the wall jet region as the nozzle-to-plate distance of the impinging jet was increased.

The three-dimensionality of the structures causing the pressure fluctuations in both regions was characterized using the azimuthal spectra given by

$$B_{pp}(r_1, r_2 = r_1, m, \tau = 0) = \frac{1}{2\pi}\int_0^{2\pi} R_{pp}(r_1, r_2 = r_1, \Delta\theta, \tau = 0)\exp(-\mathrm{i}2\pi m\Delta\theta)\,\mathrm{d}(\Delta\theta), \tag{3.1}$$

where $R_{pp}(r_1, r_2 = r_1, \Delta\theta, \tau = 0)$ is the two-point pressure correlation on a given radius, r_1, for points separated by $\Delta\theta$ in the azimuthal direction, with time lag, τ, of zero. The azimuthal mode number is denoted by m. The results for the stagnation region and the wall jet region are shown in figure 3, with the results for $r/D = 1$ shown in both regions. The spectra in these plots have been normalized so that the sum of the modes for each radii are $(\sigma_p/0.5\rho U_o^2)^2$. The results indicate that there are significant differences between the pressure fluctuations in the stagnation region and the wall jet region. For both jets, azimuthal modes 1 to 3 make the largest contribution in the stagnation region, while azimuthal mode 0, the axisymmetric ring mode, makes a small contribution, suggesting that the more three-dimensional modes play a more significant role in the stagnation region. This was particularly true for the jet with $H/D = 4$, and consistent with the findings of Kataoka *et al.* (1982) for a jet with $H/D = 6$. In the wall jet region, azimuthal mode 0 and azimuthal mode 1 (the largest antisymmetric ring mode), make significant contributions to the spectra at $r/D = 1.0$

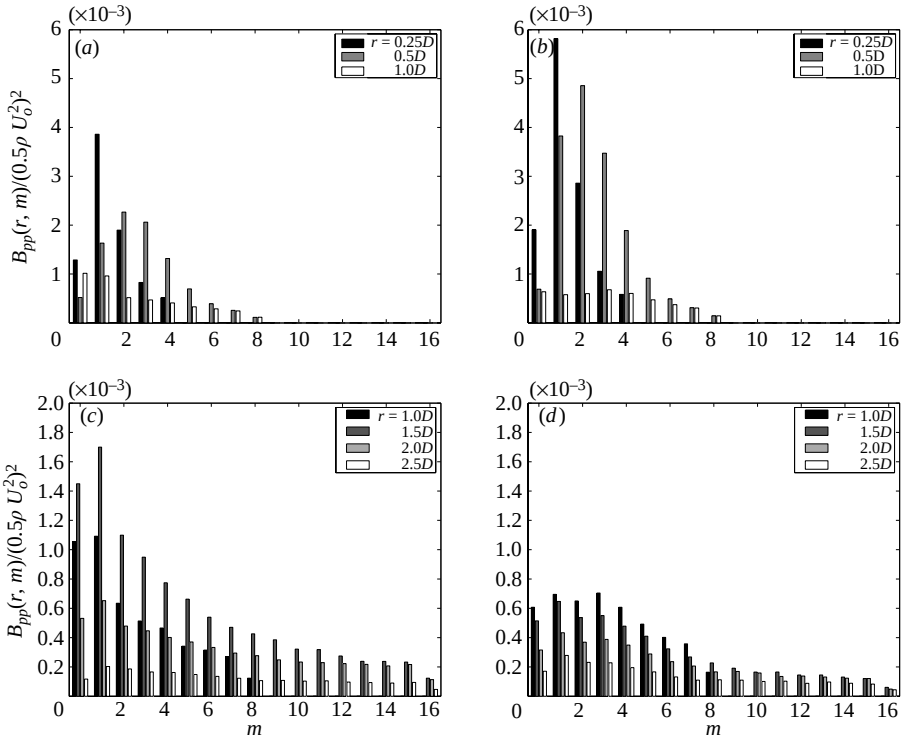

FIGURE 3. Comparison of the azimuthal spectra in (a, b) the stagnation region (from the pressure transducer measurements) and (c, d) the wall jet region (from the microphone measurements) for the impinging jets with $H/D = 2.0$ (left-hand column) and $H/D = 4.0$ (right-hand column).

and 1.5 for the jet with $H/D = 2$ indicating that there are prominent large-scale motions present in this region of the flow, as noted by Hall & Ewing (2005). The azimuthal spectra in the wall jet region were broader and less energetic for the jet with $H/D = 4$. This is not unexpected since the large-scale structures in the axisymmetric shear-layer break down as the flow evolves downstream (e.g. Liepmann & Gharib 1992; Jung *et al.* 2004). Azimuthal modes 0 and 1 still make a significant contribution to the spectra in this jet, suggesting that there are still large-scale motions present in this wall jet, but they are less prominent than in the jet with $H/D = 2$. The contributions from modes 0 and 1 decay throughout the wall jet region for the jet with $H/D = 4$ suggesting that the large-scale structures may be breaking down throughout this wall jet.

The contribution of the individual azimuthal modes to the quasi-periodic motions observed in the impinging jet can be examined using the frequency spectra of the azimuthal modes given by

$$\tilde{F}_{pp}(r_1, r_2 = r_1, m, f) = \frac{1}{2\pi}\int_0^{2\pi}\int_{-\infty}^{\infty} R_{pp}(r_1, r_2 = r_1, \Delta\theta, \tau)\exp(-\mathrm{i}(m\Delta\theta + 2\pi f\tau))\,\mathrm{d}\tau\,\mathrm{d}\Delta\theta, \tag{3.2}$$

where f is the frequency. The results for modes 0 to 5 at $r/D = 0.5$ to 2.0 are shown in figure 4. The full pressure spectra measured at each location are also shown for comparison. The spectra at $r/D = 0.5$ have a lower maximum frequency

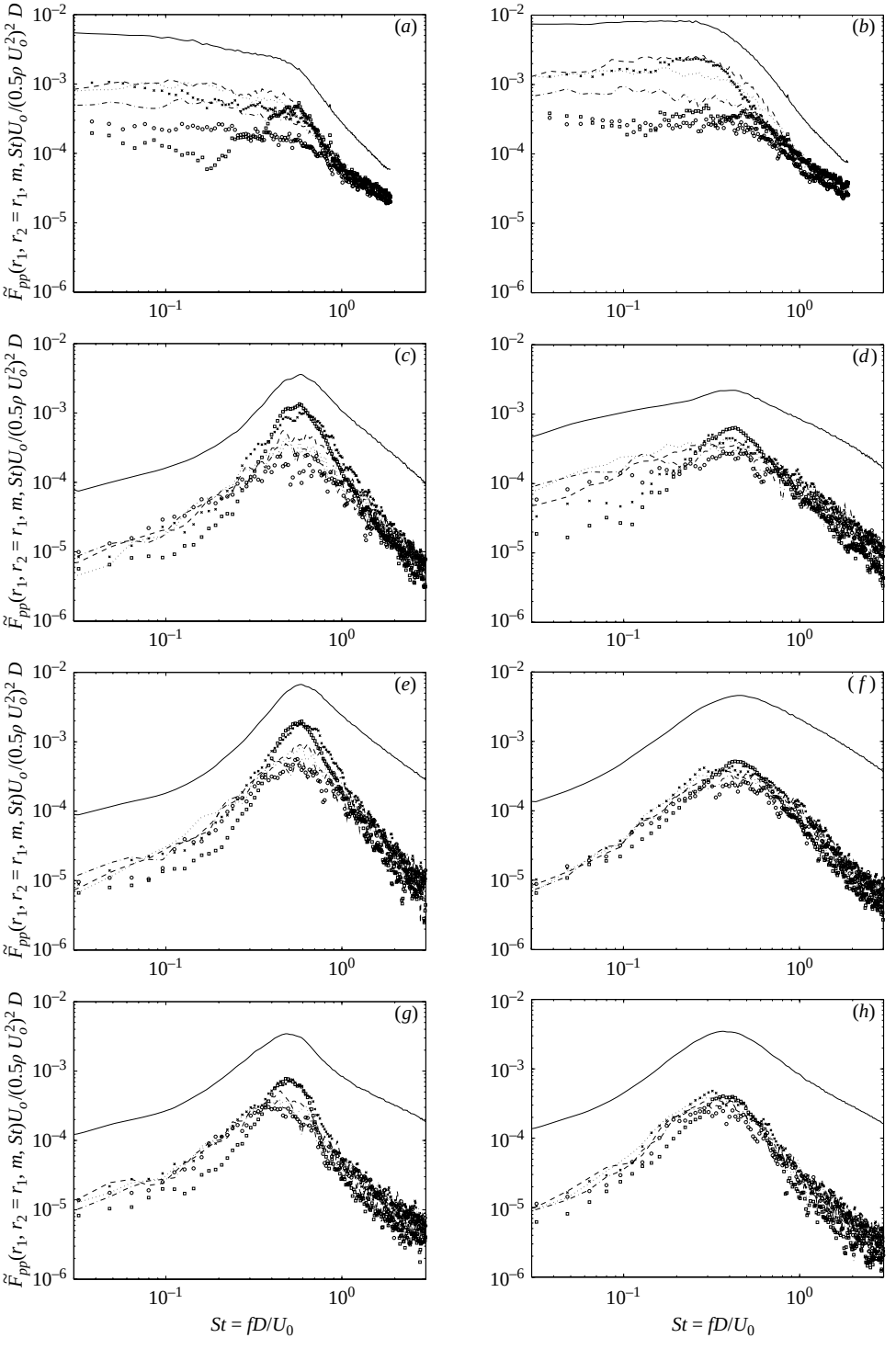

FIGURE 4. Comparison of ——, the frequency spectra of the fluctuating pressure and the contributions from azimuthal mode, □, 0, ×, 1, – – –, 2, · · ·, 3, — · —, 4, and ○, 5 at (a, b) $r/D = 0.5$ (from the pressure transducers measurements) (c, d) $r/D = 1.0$, (e, f) $r/D = 1.5$ and (g, h) $r/D = 2.0$ for the jets with $H/D = 2$ (left-hand column) and $H/D = 4$ (right-hand column).

than the other results because these were determined from the pressure transducer measurements that had a lower sampling frequency. It is clear that the pressure spectra in the stagnation region and the wall jet region are quite different. The pressure spectra in the wall jet region of both flows have distinctive peaks indicative of the passage of quasi-periodic structures, while the spectra in the stagnation region of both flows are quite broad.

The contribution from all the azimuthal modes in the wall jet region have peaks at similar frequencies, suggesting these modes are all convected at the same velocity. This will be discussed further in the analysis of the two-radii measurements. The frequency spectra for azimuthal modes 0 and 1 in the jet with $H/D = 2$ have prominent peaks at $fD/U_o = 0.5$, indicating that the pressure fluctuations associated with these modes are caused by the passage of quasi-periodic large-scale ring structures in the wall jet. The contribution from the higher azimuthal mode numbers, $m = 2$ to 5, are all similar in the radial wall region and act to broaden the peak in the conventional pressure spectra for this jet, obscuring the contributions from the largest-scale structures. The pressure spectra for the contribution of azimuthal modes 0 and 1 in the wall jet region for the case of $H/D = 4$ (i.e. figure 4*d*, *f*, *h*) do not have as prominent a peak as for the impinging jet with $H/D = 2$, indicating that the structures in the flow associated with these modes are less energetic, or are more intermittent in the jet with $H/D = 4$. In fact, the spectra for these modes change similarly to the higher azimuthal modes as the flow evolves through the wall jet region, suggesting that the largest-scale motions in the jet with $H/D = 4$ are simply convected through the wall jet region similar to the more three-dimensional motions.

The pressure spectra in the stagnation region at $r/D = 0.5$ are quite broad in both jets, but these spectra are not necessarily representative of the contribution for all of the large-scale motions. In both jets, the contributions from azimuthal mode 0 has a distinct peak at $fD/U_o = 0.5$, the same as in the spectra in the wall jet region. This suggests that the large-scale ring structures in the wall jet region are related to those in the jet shear-layer. The peak for mode 0 is much smaller in the jet with $H/D = 4$, as expected. The spectra for the contributions from azimuthal modes 1 to 3 are broad and have a lower characteristic frequency ($fD/U_o \approx 0.3$), particularly in the jet with $H/D = 4$. As a result, the characteristic frequency of the pressure spectra at $r/D = 0.5$ for the jet with $H/D = 4$ is lower than the jet with $H/D = 2$. Jung *et al.* (2004) found a similar difference between the frequency spectra of azimuthal mode 0 and the higher azimuthal modes for the streamwise velocity spectra in the axisymmetric shear-layer. This suggests that the lower-frequency motions in the stagnation region may be associated with the jet shear-layer and may not be particular to the impinging jet. There was no evidence of lower-frequency fluctuations in the wall jet region, suggesting that the low frequency azimuthal mode 1 to 3 pressure fluctuations in the stagnation region are not directly related to those in the wall jet region.

Following Hall & Ewing (2005), the convection of the structures causing the different azimuthal modes were characterized using the normalized two-radii and two-time correlation computed for each mode given by

$$\widetilde{\rho}_{pp}(r_1, r_2, m, \tau) = \frac{\widetilde{B}_{pp}(r_1, r_2, m, \tau)}{[B_{pp}(r_1, r_2 = r_1, m, \tau = 0) \cdot B_{pp}(r_1 = r_2, r_2, m, \tau = 0)]^{1/2}}, \tag{3.3}$$

where

$$\widetilde{B}_{pp}(r_1, r_2, m, \tau) = \frac{1}{2\pi} \int_0^{2\pi} R_{pp}(r_1, r_2, \Delta\theta, \tau) \exp(-\mathrm{i}m\Delta\theta)\, \mathrm{d}\Delta\theta. \tag{3.4}$$

The correlations for azimuthal modes 0, 1 and 5, and the correlations of the fluctuating wall pressure given by

$$\rho_{pp}(r_1, r_2, \Delta\theta = 0, \tau) = \frac{R_{pp}(r_1, r_2, \Delta\theta = 0, \tau)}{\left[\sigma_p^2(r_1)\sigma_p^2(r_2)\right]^{1/2}}, \tag{3.5}$$

are shown in figure 5. The correlations here are computed about the radius $r_1/D = 1.0$ in the two jets using the pressure transducer measurements, The results for $r/D \geqslant 1$ agree with similar results measured using the microphones. As noted in Hall & Ewing (2005), the two-point and two-time correlations for the fluctuating pressure decay more rapidly than the correlations for azimuthal modes 0 and 1 in the wall jet region and are better measures of the decay in the correlation of the higher modes, such as azimuthal mode 5 shown here. The correlations for azimuthal modes 0 and 1 decrease more rapidly for the jet with $H/D = 4$ indicating that the large-scales structures were breaking down more rapidly in this flow. The average convection velocity determined from the correlations were similar in both jets. The average convection speed decreased from $U_c = 0.73U_o$ in the region between $r/D = 1.0$ and 1.5 to $0.6U_o$ for $r/D = 1.5$ and 2.0 in agreement with the convection velocities of the primary and secondary vortices reported by Didden & Ho (1985), respectively. This suggests that the secondary vortices have separated from the wall in this region as discussed in Hall & Ewing (2005). There is also a larger decrease in the correlation between $r/D = 2.0$ and 2.5, consistent with this observation.

The correlations between $r/D = 1.0$ and $r/D = 0.5$ indicate that the motions that contribute to azimuthal mode 1 in the stagnation region and the wall jet regions are not that well correlated, particularly in the jet with $H/D = 4$. This differed from the results for azimuthal mode 0 that were reasonably well correlated in both jets or even the higher azimuthal modes, such as azimuthal mode 5. The frequency spectra computed from these correlations indicated that it was the lower-frequency fluctuations in the stagnation region that were not well correlated with the motions in the wall jet region, as expected. This is examined in more detail using the time-resolved simultaneous measurements of the pressure discussed below.

3.2. *Instantaneous pressure measurements*

The contribution of azimuthal modes 0 and 1 to the instantaneous pressure field at the wall was characterized by decomposing the instantaneous pressure field into azimuthal modes. This decomposition was then used to compute low-order reconstructions of the pressure field retaining only a few modes; i.e.

$$p^{(rec)}(r, \theta, t) = \sum_{m=-M}^{M} \hat{p}(r, m, t)\mathrm{e}^{\mathrm{i}m\theta}, \tag{3.6}$$

where $\hat{p}(r, m, t)$ is the Fourier coefficient of the pressure in the azimuthal direction and M is the number of modes retained in the reconstruction. Comparisons of the fluctuating pressure fields reconstructed using the contributions from azimuthal modes 0, modes 0 and 1, and all the modes (or the full pressure fields) for the jet with $H/D = 2$ are shown in figure 6. The fluctuating pressures between the neighbouring radii in the wall jet region have been interpolated by using a time lag based on the average convection velocity of the motions between the measurement points and the distance to the measurement points in order to accurately reproduce the convective character of the motions in this region. The total time interval in this figure corresponds to the nominal passage of a single structure.

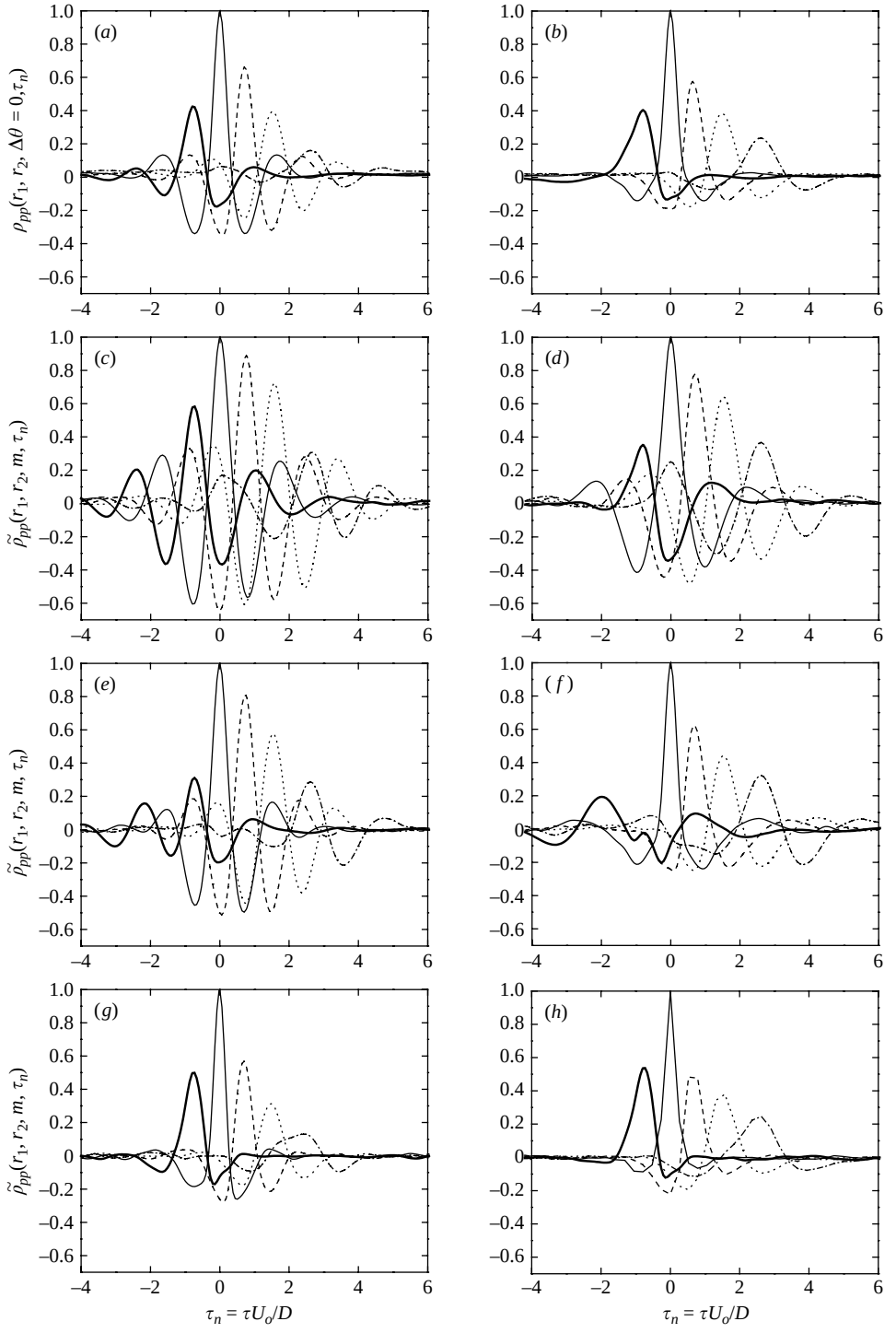

FIGURE 5. Comparison of the normalized two-point and two-time correlations between $r_1/D = 1.0$ and ——, $r_2/D = 0.5$; ——, 1.0; – – –, 1.5, ···, 2.0, and —·—, 2.5 for (a, b) the fluctuating pressure, (c, d) $m = 0$, (e, f) $m = 1$, and (g, h) $m = 5$ for the impinging jet with $H/D = 2$ (left-hand column) and $H/D = 4$ (right-hand column).

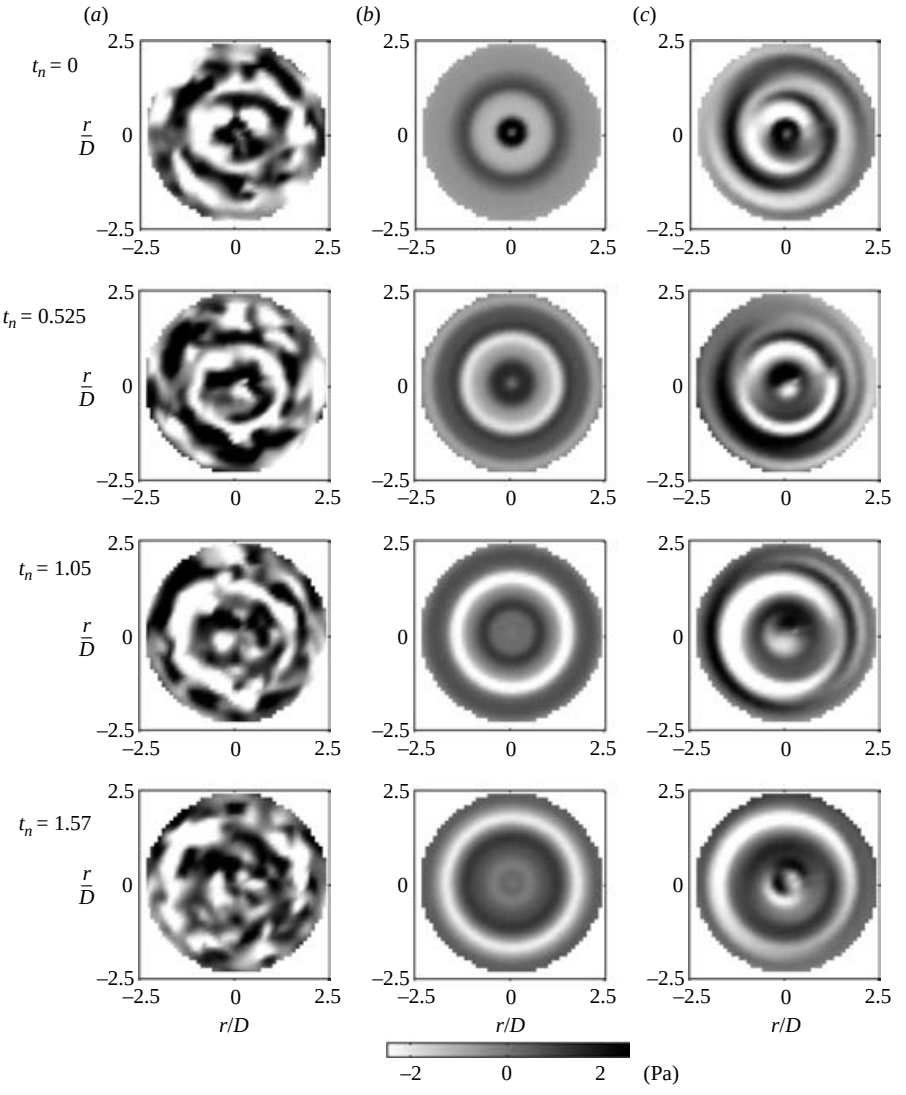

FIGURE 6. Comparison of realizations of (*a*) the instantaneous pressure, (*b*) the instantaneous pressure reconstructed using azimuthal mode 0, and (*c*) the instantaneous pressure reconstructed using azimuthal modes 0 and 1 for the impinging jet with $H/D = 2$.

It is clear from figure 6 that the large-scale events in the fluctuating pressure field are asymmetric and thus cannot be captured in the reconstructions using solely azimuthal mode 0, the axisymmetric ring mode. The asymmetry in the large-scale pressure fluctuations is well captured with the addition of only azimuthal mode 1, the largest antisymmetric mode. For example, at $t_n = tU_o/D = 0.525$ there is evidence of an asymmetric ring structure near the stagnation region in the instantaneous pressure field that evolves outward and rotates in the subsequent realizations. These events are not well captured in the reconstruction using only azimuthal mode 0, but are reasonably well represented when azimuthal mode 1 is included in the reconstruction.

There is also evidence of large asymmetric pressure fluctuations in the stagnation region that did not seem to appear at later instants in the wall jet region. This

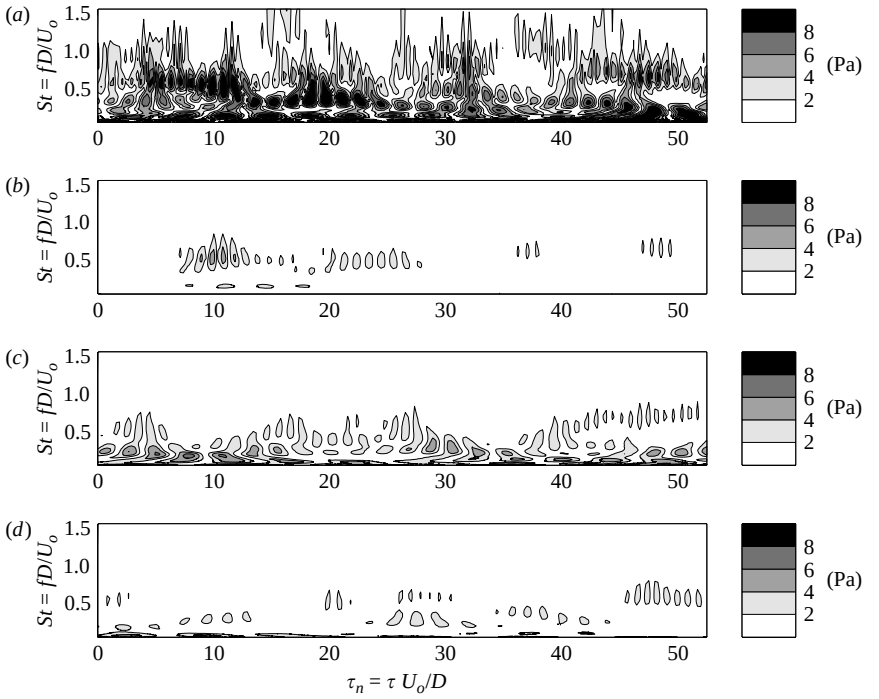

FIGURE 7. Modulus of the wavelet coefficients for (*a*) the fluctuating pressure and the contributions from azimuthal modes (*b*) 0, (*c*) 1, and (*d*) 5 in the stagnation region at $r/D = 0.5$ for the impinging jet with $H/D = 2$.

suggests that the azimuthal mode 1 fluctuations in the stagnation region are not directly linked to the mode 1 fluctuations in the radial wall jet. This event was captured in the reconstruction with azimuthal modes 0 and 1, indicating that these two modes include information about the dynamically important events in both the stagnation and wall jet regions.

The time-dependent behaviour of the pressure fluctuations in the impinging jet can be better characterized for longer durations by applying a wavelet transform to the fluctuating pressure signal or to the contribution of the different azimuthal modes to the fluctuating pressure signal. Here, the real part of a Morlet wavelet given by

$$\psi(z) = \exp(-z^2/2)\cos(5z) \tag{3.7}$$

is used in the wavelet transform; i.e.

$$P(a,\tau) = \frac{1}{\sqrt{a}} \int_{-\infty}^{\infty} p(t)\psi^* \left(\frac{(t-\tau)}{a}\right) \mathrm{d}t, \tag{3.8}$$

where a is the time scale of the wavelet, $*$ denotes complex conjugate, and τ is the temporal translation parameter. The wavelet analysis was also performed using the Mexican hat wavelet and it was found the results were relatively insensitive to the choice of wavelet.

The modulus of the wavelet coefficient for the fluctuating pressure, $P(a,\tau)$, and the contributions from azimuthal modes 0, 1 and 5 at $r/D = 0.5$ and 1.5 for the jet with $H/D = 2$ are shown in figures 7 and 8. The results are presented here by converting the time scale to one corresponding to the central frequency of the wavelet using

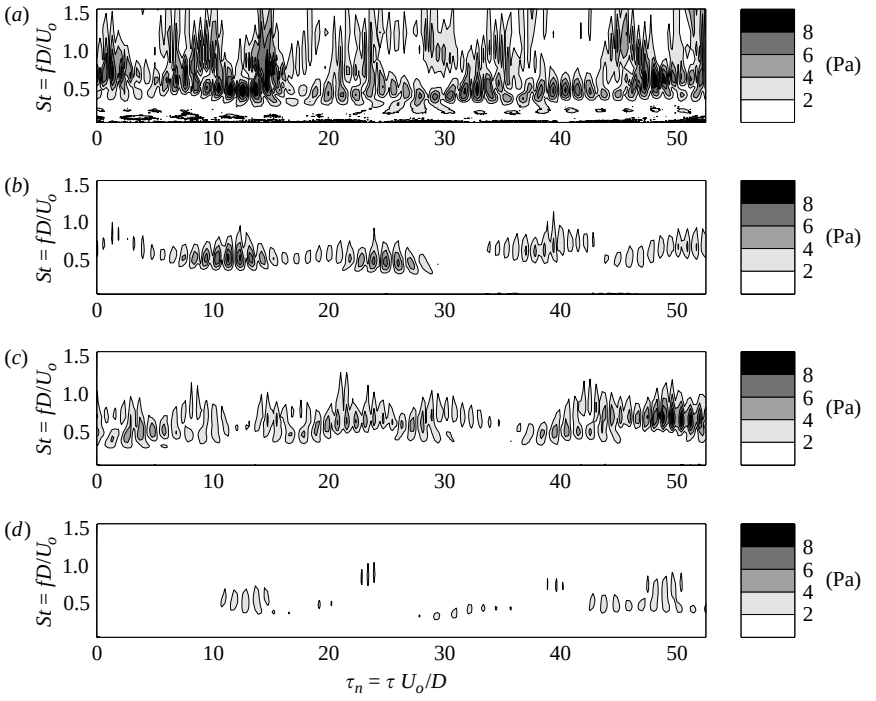

FIGURE 8. Modulus of the wavelet coefficients for (*a*) the fluctuating pressure and the contributions from azimuthal modes (*b*) 0, (*c*) 1 and (*d*) 5 in the wall jet region at $r/D = 1.5$ for the impinging jet with $H/D = 2$.

$f = 0.812/(af_s)$, where f_s is the sampling frequency. Here, the frequency and time translation parameter, τ, have been normalized using U_o and D. The results show that the fluctuating pressure signals at both radii are rich in frequency content. The characteristic frequency of the pressure fluctuations and the magnitude of the wavelet coefficients change over time, indicating that there is intermittency in the turbulent motions travelling over the plate. The intermittency of the large-scale motions is evident in the results for azimuthal mode 0, although some of the temporal periodicity in these figures is probably an artefact of the choice of a locally periodic wavelet. The characteristic frequency of the contribution from azimuthal mode 0 is centred around $fD/U_o \approx 0.5$ similar to the azimuthal frequency spectra, but the non-dimensional frequency varies between 0.3 and 0.6 in both the stagnation region and the wall jet region. The modulus of the wavelet coefficients for the contribution of azimuthal mode 1 differ in the stagnation region and the wall jet region. The modulus of the wavelet coefficients for this mode at $r/D = 0.5$ have local maxima centred around $fD/U_o \approx 0.5$ and additional local maxima centred around a lower non-dimensional frequency, similar to the frequency spectra. The wavelet coefficients at $r/D = 1.5$ in the wall jet region have local maxima around $fD/U_o \approx 0.5$ similar to the frequency spectra and azimuthal mode 0. There is no evidence of the lower-frequency motions in the wall jet region. At both locations, azimuthal mode 5, typical of the higher modes, is weak compared to azimuthal modes 0 and 1, but does appear to be intermittent as well.

The differences in the dynamics of azimuthal mode 0 and mode 1 can be seen more clearly in figures 9 and 10 where the wavelet coefficients for these modes are

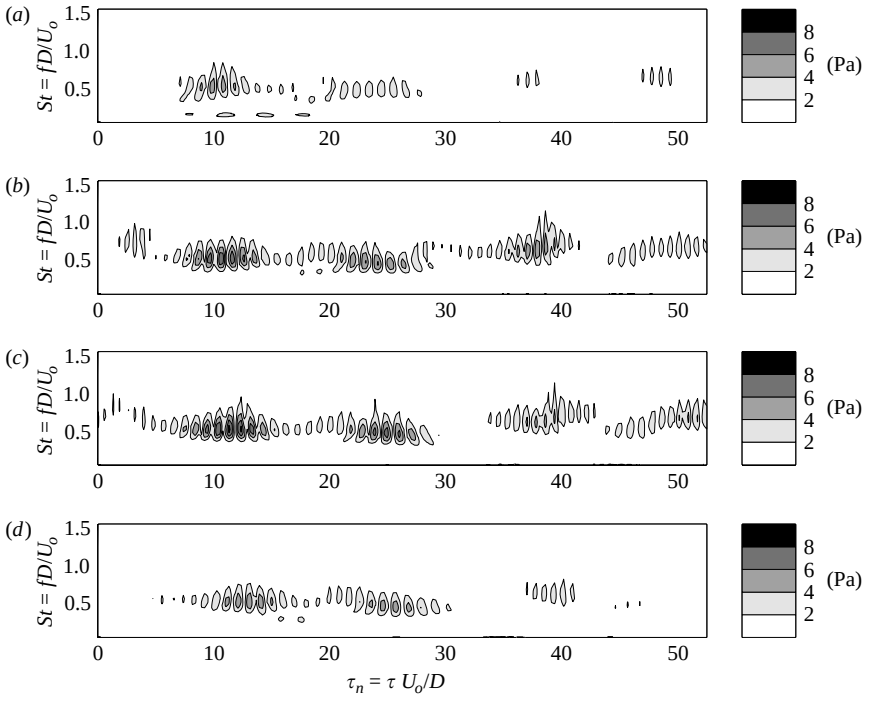

FIGURE 9. Modulus of the wavelet coefficients for the contribution from azimuthal mode 0 at (*a*) $r/D = 0.5$, (*b*) $r/D = 1.0$, (*c*) $r/D = 1.5$ and (*d*) $r/D = 2.0$ in the impinging jet with $H/D = 2$.

compared from $r/D = 0.5$ to 2.0. The magnitude of the wavelet coefficients for azimuthal mode 0 differ at the different locations, but the shapes of the distributions are similar. There is a time delay between the distributions at the different radii indicating that the motions that cause the wall pressure fluctuations with azimuthal mode 0 seem to be convected from $r/D = 0.5$ into the wall jet region. This differs from the results for azimuthal mode 1. In particular, there is a significant low-frequency contribution to azimuthal mode 1 at $r/D = 0.5$ that does not appear at $r/D = 1.0$ or at any other downstream locations in the wall jet region, suggesting that these low frequency motions are primarily related to the flow in the stagnation region. The wavelet coefficients at non-dimensional frequencies between 0.4 and 1 at $r/D = 0.5$ are often similar to those at subsequent downstream locations, suggesting that the motions causing the pressure fluctuations with frequencies similar to mode 0 may be convected from the stagnation region to the wall jet region.

The role of azimuthal mode 1 in the wall jet region was examined further by considering how the phase angle of the coefficient $\hat{p}(r, m, t)$ for mode 1 varied over time. A comparison of the phase angle for mode 1 and the modulus of the wavelet coefficients for this mode at $r/D = 1$ are shown in figure 11. There were long periods where the phase angle changed approximately linearly with time, suggesting the pressure field on the plate was rotating. This persisted for durations of up to 8 full rotations. There was no preferred direction of this rotation and there were often short interruptions in the phase.

The wavelet analysis was also applied to the measurements in the impinging jet with $H/D = 4$. The wavelet coefficients of the fluctuating pressure and modes 0,

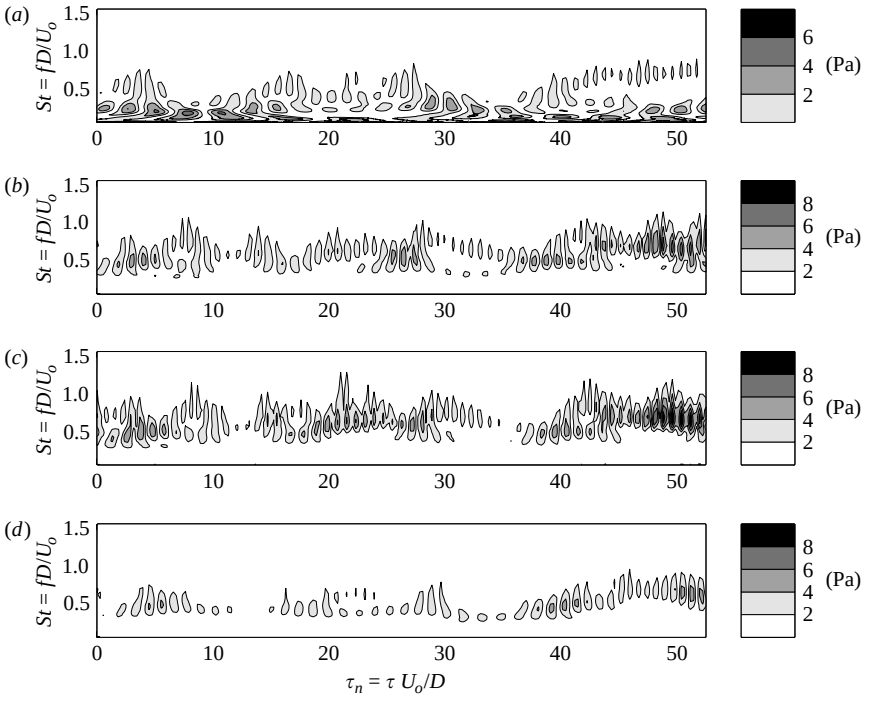

FIGURE 10. Modulus of the wavelet coefficients for the contribution from azimuthal mode 1 at (*a*) $r/D = 0.5$, (*b*) $r/D = 1.0$, (*c*) $r/D = 1.5$ and (*d*) $r/D = 2.0$ in the impinging jet with $H/D = 2$.

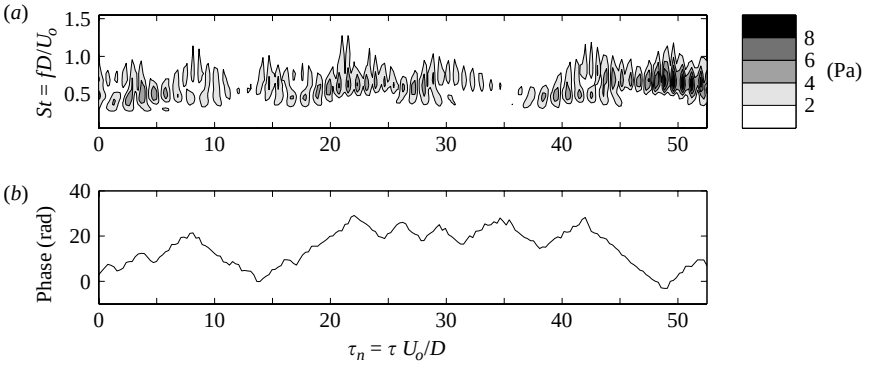

FIGURE 11. Comparison of (*a*) the modulus of the wavelet coefficient and (*b*) the phase of the contribution from azimuthal mode 1 at $r/D = 1.5$ for the impinging jet with $H/D = 2$.

1 and 5 in the stagnation region and the wall jet region of this flow are shown in figures 12 and 13. In this case, azimuthal mode 1 makes a more prominent contribution in the stagnation region. There is a large increase in the contribution from the low-frequency motions which may correspond to the refreshing motions proposed by Kataoka *et al.* (1982, 1987) for an impinging jet with $H/D = 6$. The wavelet coefficients for the contribution of azimuthal mode 1 indicate that there may be two different characteristic low-frequencies in the stagnation region: one at $fD/U_o \approx 0.3$, and a second at a much lower-frequency. There was evidence of

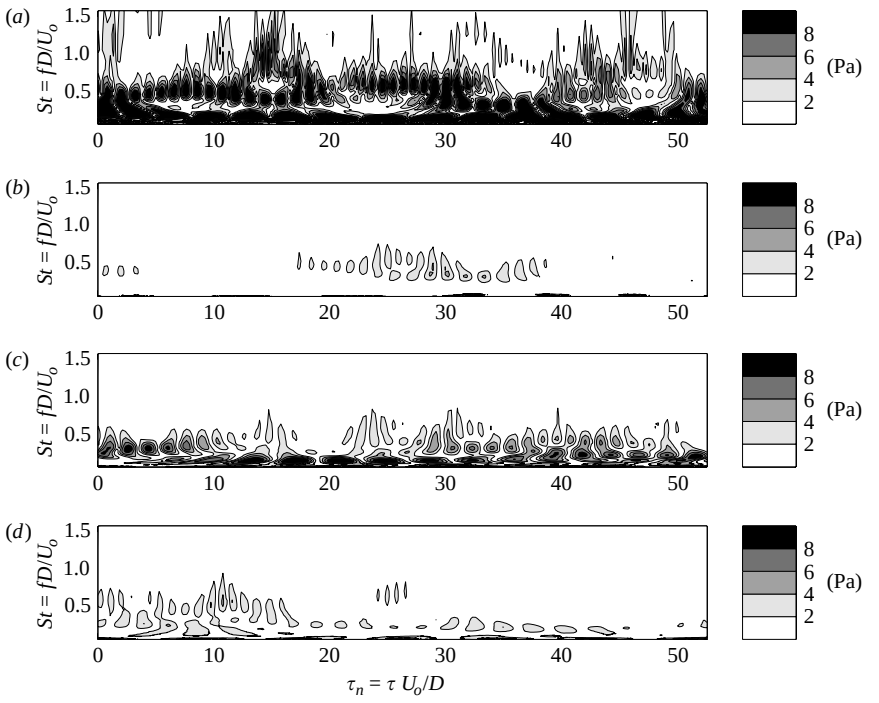

FIGURE 12. Modulus of the wavelet coefficients for (*a*) the fluctuating pressure and the contributions from azimuthal modes (*b*) 0, (*c*) 1 and (*d*) 5 in the stagnation region at $r/D = 0.5$ for $H/D = 4$.

two different low-frequencies in the jet with $H/D = 2$, though much less clearly defined. The magnitude of the coefficients for azimuthal modes 0 and 1 in the wall jet region are significantly smaller than in the jet with $H/D = 2$, but, here again, the fluctuations had characteristic frequencies centred around $fD/U_o \approx 0.5$. There is little evidence of the low-frequency fluctuations, suggesting again that the motions causing the prominent pressure fluctuations in the stagnation region and wall jet region may not be directly related. The wavelet coefficients for modes 0 and 1 in the wall jet region are not significantly more intermittent than in the jet with $H/D = 2$, indicating the large-scale structures causing the pressure fluctuations in the wall jet region become weaker as the nozzle-to-plate distance increases, rather than becoming more intermittent.

4. Summary and concluding remarks

The development of the large-scale motions in impinging jets with nozzle to plate spacings of 2 and 4 diameters was investigated using measurements of the fluctuating wall pressure. The results indicated that the behaviour of the structures in the stagnation and wall jet regions differed in the impinging jet. The pressure fluctuations in the stagnation region were more three-dimensional, similar to the findings of Kataoka *et al.* (1982, 1987) for a jet with $H/D = 6$, with azimuthal modes 1 to 3 making the most prominent contributions in the jets studied here. The frequency spectra for these modes in the stagnation region were broad and a wavelet analysis indicated that the motions had two different ranges of characteristic frequencies, one

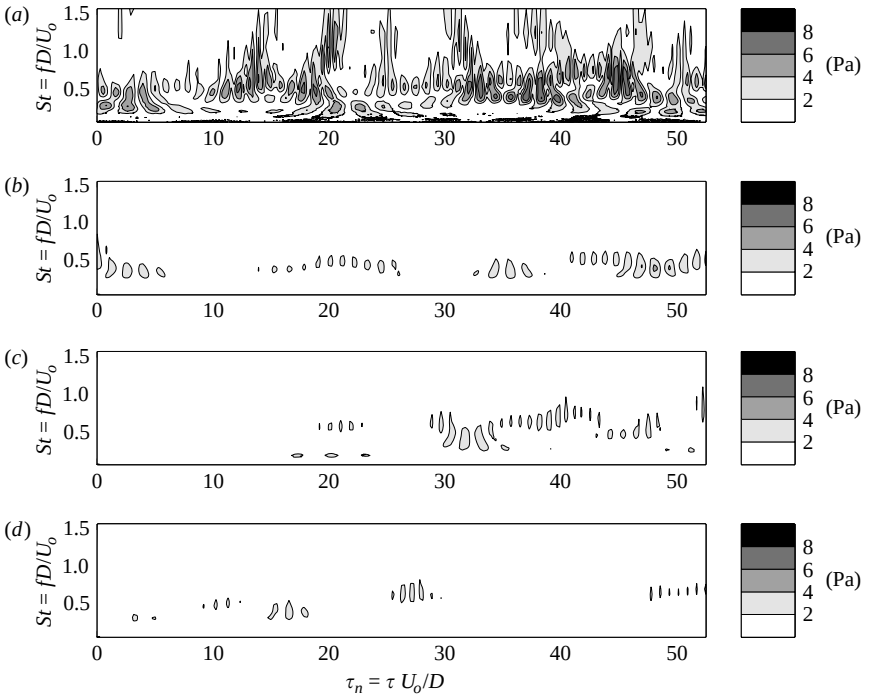

FIGURE 13. Modulus of the wavelet coefficients for (*a*) the fluctuating pressure and the contributions from azimuthal modes (*b*) 0, (*c*) 1 and (*d*) 5 in the wall jet region at $r/D = 1.5$ for impinging jet with $H/D = 4$.

corresponding to the azimuthal mode 0 fluctuations in the jet and a second at a lower-frequency range. The frequency spectra for modes 1 to 3 reported here are similar to those for velocity measurements in the axisymmetric shear-layer of a free jet reported by Jung *et al.* (2004) and others, suggesting that the lower-frequency motions may be associated with oscillations in the jet shear-layer and are not necessarily particular to the impinging jet. These oscillations may be associated with what many investigators refer to as the helical mode in the free jet.

The measurements in the wall jet region indicated that there were large-scale ring structures present in this region that had a characteristic frequency similar to the vortex rings in the stagnation region. The pressure fluctuations were asymmetric in this region with azimuthal modes 0 and 1 making similar contributions. This asymmetry of the large-scale structures included large periods of rotation that could act to promote the heat transfer in the wall jet region by periodically moving regions of large near-wall turbulence. The azimuthal mode 1 fluctuations in the wall jet region had a similar frequency to azimuthal mode 0 and there was little or no evidence of low-frequency motions in this region. Thus, the azimuthal mode 1 fluctuations in the wall jet region are probably associated with an asymmetric interaction between the ring structures formed in the jet shear-layer and the wall, and do not seem to be directly related to the prominent large-scale fluctuations in the stagnation region. The asymmetry in the development of the ring structures may be less prominent for impinging jets exiting contoured nozzles, since the structures formed in the shear-layers of these jets appear to be less asymmetric than those in free jets exiting long pipes (see Schefer *et al.*1994; Mi, Nobes & Nathan 2001). Landreth & Adrian (1990)

observed, though, that there was still significant asymmetry in the vortical structures in an impinging jet exiting a contoured nozzle.

The change in the contributions from the large-scale fluctuations in the two regions differed as the distance between the nozzle and plate varied. The contribution from the large-scale three-dimensional modes in the stagnation region increased in magnitude as the nozzle-to-plate distance increased. This probably causes the enhancement in the heat transfer produced by the impinging jet in this region when the nozzle-to-plate distance is increased. The contribution from the large-scale motions in the wall jet region decrease in prominence as the nozzle-to-plate distance increases and this too probably explains the decrease in the secondary peak of the heat transfer in this region. The differences in the contributions from the large-scale structures in the two regions, again, suggest that the structures causing the prominent fluctuations in the stagnation region and the wall jet regions are not directly related. The different mechanisms in the stagnation and wall jet regions of the impinging jet may also explain differences in the turbulent flow field in these regions. In particular, the maximum in the turbulence intensity in the stagnation region increases as H/D increases, while the turbulence intensity in the wall jet region decreases for the same change in H/D (Cooper *et al.* 1993).

The authors would like to acknowledge the financial support of the Natural Sciences and Engineering Research Council of Canada. The authors are also grateful for the assistance of N. Gao with the statistical measurements and Z. Xu, H. Hangan and G. Dafoe at the University of Western Ontario's Boundary Layer Wind Tunnel Facility with the simultaneous measurements of the pressure field. The authors would also like to thank S. Cansfield and S. Goldstein for constructing the experimental facility used in this investigation. Finally, the authors would like to thank H. Naguib for his comments on the work.

REFERENCES

Citriniti, J. H. & George, W. K. 2000 Reconstruction of the global velocity field in the axisymmetric mixing layer utilizing the proper orthogonal decomposition. *J. Fluid Mech.* **418**, 137–166.

Cooper, D., Jackson, D. C., Launder, B. E. & Liau G. X. 1993 Impinging jet studies for turbulence model assessment. I. Flow-field experiments. *Intl J. Heat Mass Transfer* **36**, 2675–2684.

Didden, N. & Ho, C. 1985 Unsteady separation in a boundary layer produced by an impinging jet. *J. Fluid Mech.* **160**, 235–256.

Doligalski, T. L., Smith, C. R. & Walker, J. D. A. 1994 Vortex interactions with walls. *Annu. Rev. Fluid Mech.* **26**, 573–616.

Fairweather, M. & Hargrave, G. K. 2002 Experimental investigation of an axisymmetric, impinging turbulent jet. 1 Velocity Field. *Exps. Fluids* **33**, 464–471.

Gao, N., Sun, H. & Ewing, D. 2003 Heat transfer to impinging round jets with triangular tabs. *Intl J. Heat Mass Transfer* **46**, 2557–2569.

Gogineni, S. & Shih, C. 1997 Experimental investigation of the unsteady structure of a transitional plane wall jet. *Exps. Fluids* **23**, 121–129.

Hall, J. W., Ewing, D., Xu, Z. & Hangan, H. 2003 The dynamics of the large-scale turbulent structures in the impinging round jet. In *Proc. 2003 ASME Intl Mech. Engng Congress & Exposition, Washington, DC, USA*. IMECE2003-42812.

Hall, J. W. & Ewing, D. 2005 The development of the large-scale structures in round impinging jets exiting long pipes at two Reynolds numbers. *Exps. Fluids* **38**, 53–61.

Hall, J. W., Gao, N. & Ewing, D. 2002 The three-dimensional evolution of the large-scale structures in the impinging round jet. In *Proc. ASME Fluids Engng Div. Summer Meeting, Montreal, Quebec, Canada*. FEDSM2002-31419.

Ho, C. & Nosseir, N. S. 1980 Large-coherent structures in an impinging jet. In *Turbulent Shear Flows 2* (ed. J. S. L. Bradbury, F. Durst, B. E. Launder, F. W. Schmidt & J. H. Whitelaw), pp. 297–304. Springer.

Ho, C. & Nosseir, N. S. 1981 Dynamics of an impinging jet. Part 1. The feedback phenomenon. *J. Fluid Mech.* **105**, 119–142.

Jung, D., Gamard, S. & George, W. K. 2004 Downstream evolution of the most energetic modes in a turbulent axisymmetric jet at high Reynolds number. Part 1. The near-field region. *J. Fluids Mech.* **514**, 173–204.

Kataoka, K., Kamiyama, Y., Hashimoto, S. & Komai, T. 1982 Mass transfer between a plane surface and an impinging turbulent jet: the influence of surface-pressure fluctuation. *J. Fluid Mech.* **119**, 91–105.

Kataoka, K., Suguro, M., Degawa, H., Maruo, K. & Mihata, I. 1987 The effect of surface renewal due to large-scales eddies on jet impingement heat transfer. *Intl J. Heat Mass Transfer* **30**, 559–567.

Landreth, C. C. & Adrian, R. J. 1990 Impingement of a low-Reynolds number turbulent circular jet onto a flat plate at normal incidence. *Exps. Fluids* **9**, 74–84.

Liepmann, D. & Gharib, M. 1992 The role of streamwise vorticity in the near-field entrainment of round jets. *J. Fluid Mech.* **245**, 643–668.

Mi, J., Nobes, D. S. & Nathan, G. J. 2001 Influence of jet exit conditions on the passive scalar field of an axisymmetric free jet. *J. Fluid Mech.* **432**, 91–125.

Nosseir, N. S. & Ho, C.-M. 1982 Dynamics of an impinging jet. Part 2. The noise generation. *J. Fluid Mech.* **116**, 379–391.

Popiel, C. O. & Trass, O. 1991 Visualization of a free and impinging round jet. *Expl. Thermal Fluid Sci.* **4**, 253–264.

Schefer, R. W., Kerstein, A. R., Namazian, M. & Kelly, J. 1994 Role of large-scale structures in a nonreacting turbulent CH_4 jet. *Phys. Fluids* **6**, 652–661.

Sun, H. 2002 The effect of initial conditions on the development of the three-dimensional wall jet. PhD thesis, McMaster University, Hamilton, Ontario, Canada.

Tsobokura, T., Kobayashi, T., Taniguchi, N. & Jones, W. P. 2003 A numerical study on the eddy structures of impinging jets excited at the inlet. *Intl J. Heat Fluid Flow* **24**, 500–511.

Viskanta, R. 1993 Heat transfer to impinging isothermal gas and flame jets. *Expl. Thermal Fluid Sci.* **6**, 111–134.

Walker, J. D. A., Smith, C. R., Cerra, A. W. & Doligalski, T. L. 1987 The impact of a vortex ring on a wall. *J. Fluid Mech.* **181**, 99–140.

Webb, B. W. & Ma, C. F. 1995 Single-phase liquid jet impingement heat transfer. *Adv. Heat Transfer* **26**, 105–217.